An automated laboratory rainfall simulation system with controlled rainfall intensity, raindrop energy and soil drainage

C.T. Hignett [a], S. Gusli [b,c], A. Cass [b,*], W. Besz [b,c]

[a] *CSIRO Division of Soils, PMB2, Glen Osmond, S.A. 5064, Australia*
[b] *Cooperative Research Centre for Soil and Land Management, Private Bag 2, Glen Osmond, S.A. 5064, Australia*
[c] *Department of Soil Science, University of Adelaide, Adelaide, Australia*

Abstract

We report on the construction and operation of a laboratory rainfall simulator capable of producing rainfall of variable raindrop kinetic energy flux at the soil surface by varying raindrop size, drop height and rainfall intensity. The simulator was designed to study breakdown of soil aggregates during simulated rainfall under conditions of variable soil and rainfall factors. During tests, eight soil samples, 104 mm in diameter and 50 mm deep were accommodated on drained beds with controlled suction at the base (drainage). Ponded water on the soil surface was removed by suction (runoff), preventing interaction between water on the surface and rain. Depth of rainfall, runoff and drainage were measured to within 0.5 mm, at 1 min intervals, by electronic sensors and the data stored in a computer. The soil samples were surrounded by a large drained bed covered with a thin layer of test soil which served as an exchange bed, preventing splash loss of surface material from the sample during rainfall tests. These features enabled small quantities of soils to be tested under simulated field conditions (absence of ponding, profile drainage, no net loss of surface soil) without the complex interactions between applied rain and the artifactual effects of ponded surface water and excessively saturated soil often present in field and laboratory simulators with undrained target areas.

Keywords: Rainfall simulation; Data acquisition; Infiltration; Runoff; Drainage

1. Introduction

Natural rainfall displays a loose correlation between the intensity of a storm, the drop size and the energy of raindrops (Kinnell, 1981, 1987; Rosewell, 1986). Furthermore, drop

---

* Corresponding author.

size varies because larger drops form in the centre of a cloud where they accrete more water as they are circulated in updraughts (Horton, 1948; Eigel and Moore, 1983). Larger raindrops have a higher terminal velocity falling through air (Horton, 1948) further increasing the impact energy of these drops on the soil surface. Frequently, larger drops tend to fall near the most intense part of a storm, near the middle of the event (Laws and Parsons, 1943). Maximum effect on bare soil surfaces exposed to the rain is registered at this time.

Qualitative relationships between rainfall energy and soil damage have been established for some time. However, the effects of drop size and kinetic energy of rain on soil surfaces have not been studied in quantitative detail, in part because of the difficulty of measuring rapid changes in water balance at the soil surface. Rainfall simulators used to measure effects of rain on soil structure have been one of two types: (1) simulators designed to produce large drops at near terminal velocity, usually delivered from modules with arrays of hypodermic needles and falling 5 m or more (e.g. Walker et al., 1977); (2) simulators of the spinning disk type (Morin et al., 1967) which produce rain dominated by large drops falling at very high instantaneous intensity but pulsed to give lower overall intensity. These approaches are appropriate to erosion studies which have been the concern of most workers in this field.

Preliminary work at this laboratory indicated that a number of important measures of soil structural behaviour could be found if low energy or variable energy rain was used (Hignett, 1991). Among them, a minimum rainfall energy was identified, below which many soils do not break down, irrespective of rain depth even at very high rainfall intensity. Low-energy simulated rainfall applied to beds of air-dry aggregates induced different degrees of surface breakdown and rainfall runoff that could be more effectively correlated with different soil and land management systems than aggregate wet sieving. These hydrological responses also had more direct relevance to behaviour of the soil in the field. More recent work (Gusli et al., 1995) with hardsetting soils has found a range of quite unexpected interactions between rainfall energy flux density and the disruption of soil aggregates due to rainfall and wetting rate.

Rainfall simulators used in field erosion studies need to have uniform distribution of drops over a large area (~ 1 m^2). Spinning disk and spray nozzle types achieve this requirement but suffer from the disadvantage that raindrop energy is constant and high (~ 32 J m^{-2} mm^{-1}) irrespective of the intensity of application. In such sprays, the nozzle flow and drop size distribution remain constant and variation in intensity is achieved by intercepting the stream before it reaches the soil. A consequence of this combination of factors is that while higher intensity produces more runoff in a given time, the rate of change of infiltration rate of water into the soil surface is a function of accumulated rain depth and is independent of the intensity of applied rain (Morin and Benyamini, 1977). This contradicts numerous field observations which show that low intensity natural rainfall does less damage to surface soil structure, per unit depth of rain, than higher intensity rain.

This paper describes a laboratory rainfall simulator which was largely free of the limitations discussed above. It could simulate rainfall at one of two drop sizes, a range of fall heights and with controlled intensity so that soil aggregate breakdown could be studied in relation to a wide range of rainfall factors under laboratory conditions. Of particular importance was the control of rainfall energy flux density which could be varied by independently varying raindrop energy and rainfall intensity. Incorporation of electronic sensors in various

parts of the simulator allowed detailed measurements of rainfall intensity, runoff and drainage, producing new insights into the effects of rain on surface sealing and soil compaction.

2. Methods and materials

2.1. Rainfall module design

A diagram of the rainfall simulator is presented in Fig. 1. The housing was a 1140 mm × 1400 mm enclosure, 3800 mm high constructed on a box frame of 50 mm square section (16 gauge) galvanised tubing. Opening windows on opposite sides allow access to the sample area while the rest of the sides were covered with thin galvanised iron or transparent PVC sheeting to allow light access. A waterproof tray of heavier gauge galvanised sheeting just above the floor provided a solid base and extended outside the frame to intercept any water escaping through the windows.

The rain module (Fig. 1) was constructed according to Walker et al. (1977) from two rectangular transparent acrylic containers 500 mm × 1000 mm × 70 mm high disposed side by side to cover an area of 1 m². The total capacity of the module was 0.047 m³. The acrylic sheets, of 6 mm thickness, were glued and screwed together and the upper sheet was attached via removable bolts and a rubber gasket to allow access to the interior. Emitters were formed from hypodermic needles (23 gauge, 31.75 mm long) inserted into an array of holes, of 25
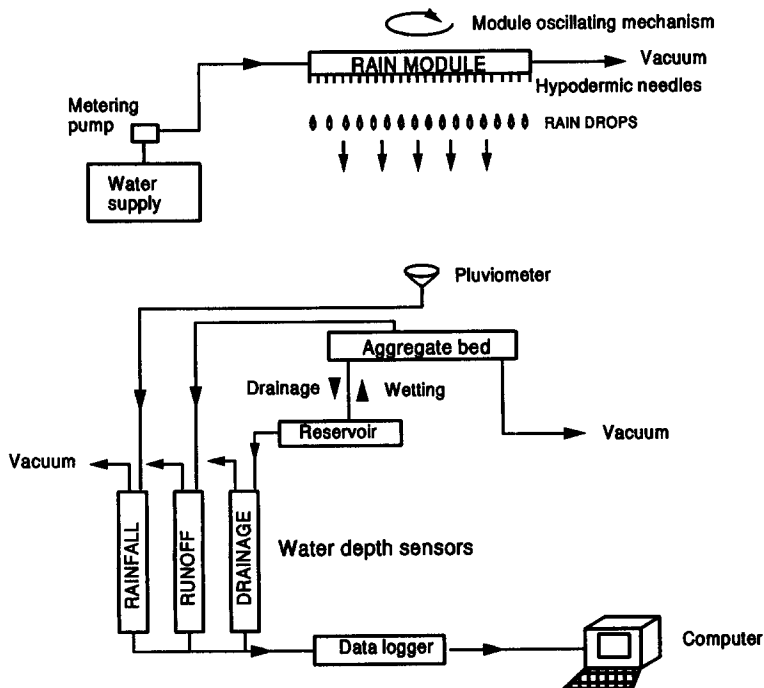

Fig. 1. Schematic diagram of laboratory rainfall simulator.

mm spacing, drilled into the lower surface of the modules (total of 1600 emitters/m^2). These emitters produced raindrops of 2.7 mm diameter. An emitter with a different drop size (5.1 mm diameter) was made by placing the hypodermic needle sheath, after sectioning the tip to create an aperture, over the needle. Raindrops of a range of sizes can be created by varying the type of needles and their receptacles. The modules were originally designed to operate in the rainfall simulator described by Walker et al. (1977).

The rectangular tanks were mounted within a steel frame to form a module that could deliver rainfall of a given drop size, over an area of 1 m^2. The module was mounted on four rollers and an electric motor and eccentric drive were used to oscillate the module at a frequency of 0.23 s^{-1} with a horizontal circular motion over a path of 100 mm diameter. This facility ensured that raindrops from individual needles were distributed evenly over the soil target area. The height of the rain module was adjustable from 0.17 to 2.54 m from the surface of the target soil bed. This height range could produce rainfall kinetic energy from 1.6 to 16.6 J m^{-2} mm^{-1} for 2.7 mm diameter drops and from 1.6 to 19.9 J m^{-2} mm^{-1} for 5.1 mm diameter drops (Table 1).

2.2. Rainfall module operation

While the modules were being filled and adjusted, soil samples in the simulator were covered to prevent water reaching the soil. Deionised water was pumped from a constant head reservoir while a small vacuum (1.0 kPa) was applied to the modules, counteracting pressure due to filling, minimising air entrapment and preventing water flow from the needles during filling. When full, the vacuum was released and water was briefly (~ 4 min) pumped at high rate through the needles to clear them of obstructions such as air bubbles or algal growth. During this time needles were checked for delivery of water and any remaining obstructions were cleared by applying a vacuum on the needle with a hypodermic syringe.

A peristaltic pump (Masterflex, 6 to 600 rpm) was used to deliver water from a constant head tank to the module in order to achieve a constant, controllable, delivery rate (rainfall intensity) from the needles. A pluviometer, placed on the soil cover, recorded rainfall intensity electronically and the output was used to manually adjust the delivery rate of the peristaltic pump to the desired rainfall intensity. Rainfall intensity was monitored throughout the test using a pluviometer in the test bed. Intensity was relatively constant during all tests especially if in excess of 40 mm h^{-1}, but required some adjustment during the test at lower intensities.

When the desired rainfall intensity has been set and checked, the test bed cover was removed, starting the experiment.

2.3. Test bed construction

The aggregate test bed (Figs. 1 and 2) was mounted on a railed platform, 680 mm above the floor such that the entire sample holder could be slid out of the simulator for sample preparation and post-rainfall measurements. The platform was 180 mm high mounted on a metal frame 500 mm above the drip tray on the base of the simulator. Fig. 2 is a diagram of the soil test bed in its most commonly used configuration.
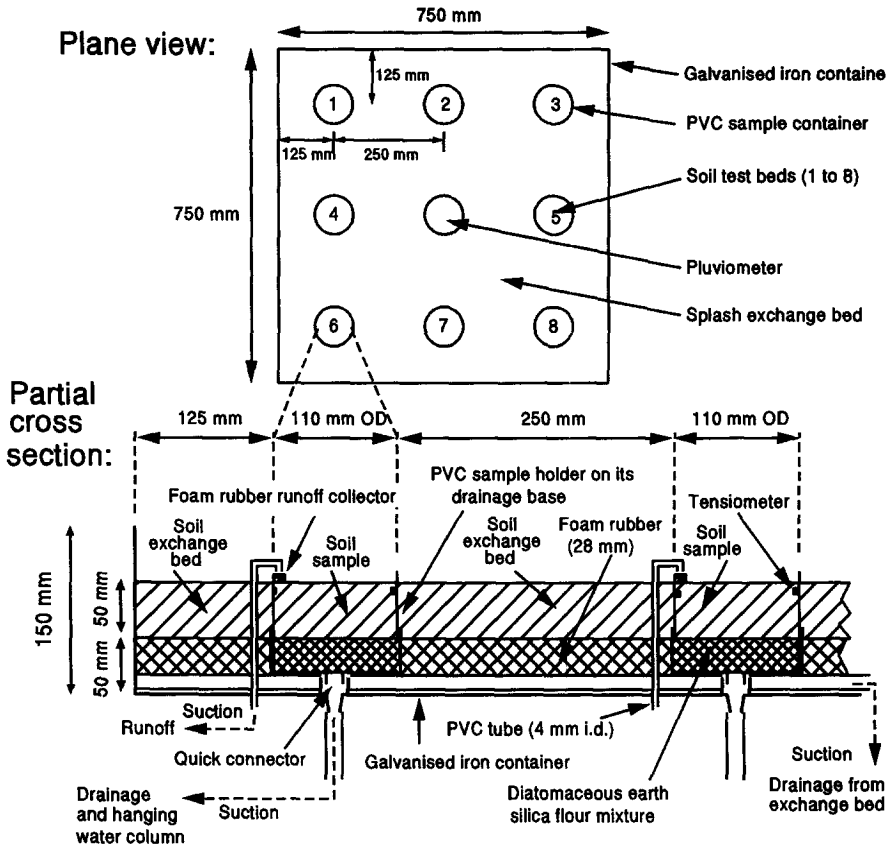
Plane view:

Fig. 2. Vertical and cross-sectional views of the rainfall aggregate bed.

The importance of an exchange bed for splash export and import with the soil samples has been shown by, among others, Moss and Watson (1991). Accordingly, the soil sample beds were surrounded by a large splash exchange bed (Fig. 2). The splash exchange bed was made from 50 mm thick foam plastic, supporting a thin layer of soil, laid on top of a network of perforated PVC tubes under vacuum of 3 kPa, to provide drainage. The foam plastic reduced the quantity of exchange bed soil required and filtered coarse particles from the drainage system. Soil similar to that under test was used in the exchange bed. The exchange bed and test soil samples were set at a slope of 3% to facilitate runoff collection.

Sample holders were constructed from PVC tubing (54 mm high, 110 mm outside diameter, 3 mm wall) with an outside facing knife edge (30 degree angle) machined on the upper rim and a disc of PVC mesh (4 mm openings) was glued to the base of the cylinder. A standard PVC pipe end cap fitting (inside diameter 110 mm, height 28 mm) was used as a drained base for the sample holder. A plastic spigot was inserted into a hole (10 mm diameter) in the centre of the end cap. The end cap was filled with a slurry of equal proportions, by mass, of diatomaceous earth and silica flour (400 G). The drainage base could hold a suction up to 11.8 kPa without air entry and had a reasonably high saturated

hydraulic conductivity (17 mm h^{-1}). This mixture was used in preference to ceramic plates because it was inexpensive, discardable when contaminated with silt and clay from the sample and provided means to vary the subsample drainage rate by varying the proportions of the mixture. Two layers of open-weave synthetic cloth were placed on top of the drainage bed to filter some silt and clay emanating from the soil sample, so prolonging the useful life of the drainage bed.

The sample holder was placed on the cloth covering the drainage bed and held in firm contact with a broad rubber band. The assembly of drainage base and sample holder was inserted into an aperture in the test bed via the drainage spigot. This provided a connection between the drainage base and a hanging water column below the simulator which was designed to drain the soil sample being tested. A thin layer of diatomaceous earth was spread over the mesh on the bottom of the sample holder to provide better hydraulic contact between the soil sample and the top of the drainage base. Hydraulic contact was established by filling the drainage system from the sample holder. A suction of 3 kPa was established on the base of the sample and maintained throughout the test.

2.4. Test bed operation

Soil samples were prepared by air drying, gently crushing large aggregates and passing the soil through a 5 mm sieve. The soil sample was rapidly dumped into the sample holder to minimise particle segregation. The surface aggregates were lightly stirred to redistribute aggregates and reduce any extreme surface irregularities. In the case of tests on dry soil, rainfall was applied immediately after this. However, rainfall could also be delayed until the soil surface was wetted by upward flux of water from the hanging water column attached to the base of each test sample. Suctions of up to 5 kPa were possible.

Soil samples and test bed were covered until rainfall intensity was correctly adjusted and data logging equipment was operating satisfactorily, at which time the cover was removed and the test commenced. During the test, changes in cumulative rainfall, runoff and drainage were measured automatically once per minute. Water accumulating on the surface of the sample (runoff) was removed by vacuum through a small (10 mm square) plastic foam element (Wace and Hignett, 1991) and delivered to a tube equipped with a capacitance water depth sensor (Ross, 1983). Air entry suction of the plastic foam was about 5 mm of water, so that minimum suction was transferred to the soil surface, but any free water touching the foam element was extracted. Rainwater collected from the pluviometer was delivered under vacuum to a capacitance water depth sensor. Water draining through the bottom of the test sample was collected and delivered by gravity to capacitance water depth sensors via a hanging water column of 300 mm.

2.5. Data collection

Water depth sensors (Fig. 3) were constructed using the electronic circuitry and the teflon-coated brass rod (500 mm length, 1 mm diameter) obtained from commercial bore-hole water depth sensors (Dataflow Systems). The electronics and rod were inserted into the base of a transparent acrylic tube (26 mm internal diameter for runoff and drainage, 40 mm for the pluviometer) (Fig. 3). Fine wire was wound loosely around the outside of the
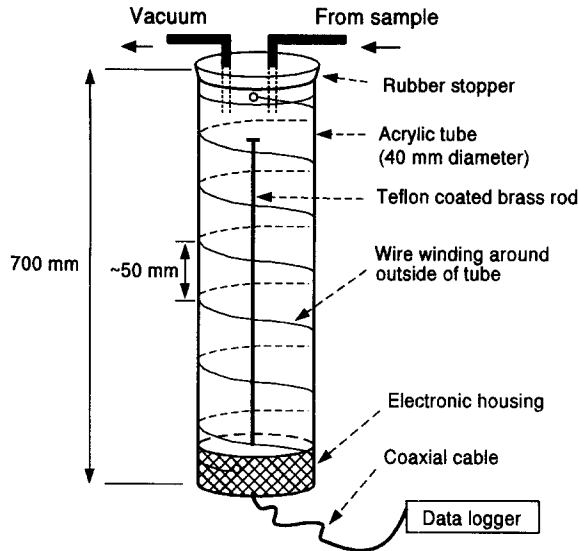
Fig. 3. Configuration of the capacitance water depth sensors.

tube and covered with aluminium foil. This assembly enabled reliable measurement of water depths with a sensitivity better than 0.5 mm over the lower half of the capacity of the acrylic tube. Sensor output was a frequency signal which was calibrated against water depth in the cylinder (Fig. 4). Below 40 Hz the sensitivity of the sensor was lower than 0.8 mm/Hz, increasing rapidly above this frequency. Accordingly, the latter condition was always avoided during tests.

$$d_{rain} = -12.25 + 2645 \, S^{-1}$$
$$\sigma_{x,y} = 0.6959 \text{ mm} \qquad r^2 = 0.999$$

$$d_{runoff} = -6.409 + 1322 \, S^{-1}$$
$$= d_{drainage}$$
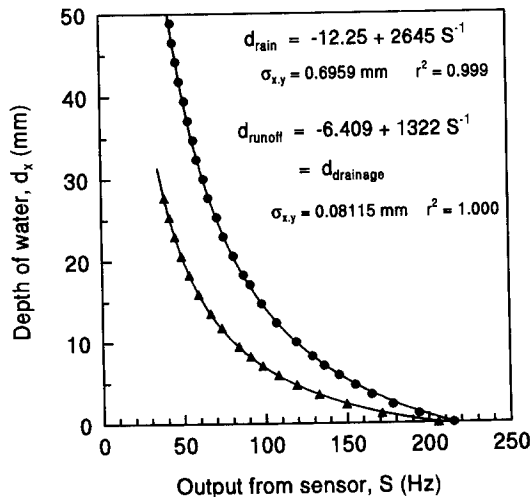$$\sigma_{x,y} = 0.08115 \text{ mm} \qquad r^2 = 1.000$$

Fig. 4. Calibration curves for the rainfall (circles) and the mean ($n = 16$) runoff and drainage (triangles) depth gauges and fitted functions (solid lines). Standard errors of the means are smaller than the triangular symbols used to show the data.
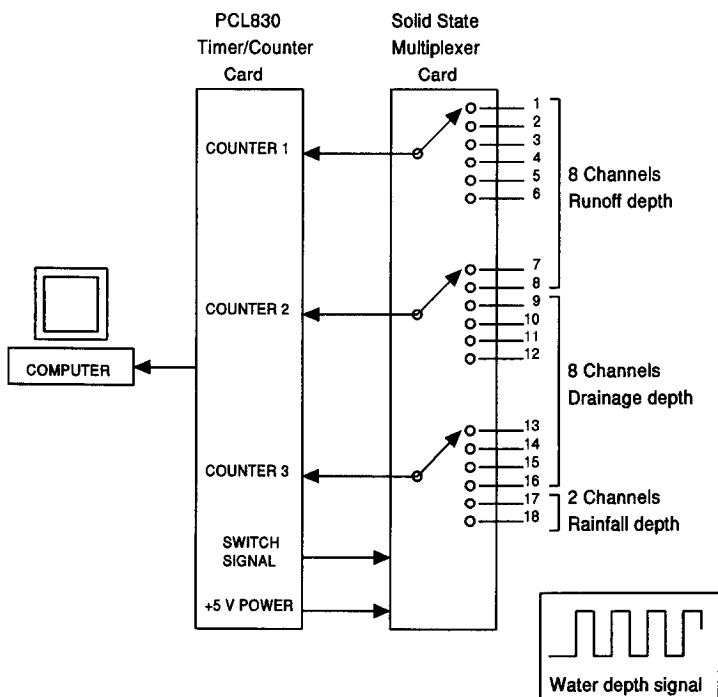
Fig. 5. Block diagram of the electronic circuit used to capture and log depth of runoff, drainage and rainfall from the rainfall simulator.

A personal computer and custom software were used to interrogate and log the output from the sensors measuring rainfall intensity, runoff and drainage from the test samples. A commercially available PC timer/counter card (PCL830) was configured as a 3-channel frequency counter (Fig. 5). A solid-state multiplexer was built to select a further 6 channels for each of the 3 frequency inputs to the PCL830 card, thus allowing 18 channels of measurement.

The modified capacitance water depth sensors were connected to each of the channels as shown in Fig. 5. Sixteen channels were dedicated to each of runoff and drainage from the eight soil sample holders and two to rainfall intensity via the pluviometer. The two channels devoted to logging rain intensity were used alternately in order to remain within the range of maximum sensitivity of the water depth sensors, the operator draining whichever one was not in use at any given time.

Depth of water in each sensor was read every minute, the data stored in RAM and displayed on the screen. Rainfall intensity was calculated each minute, stored in RAM and displayed on the screen together with an updated average of the previous ten readings. At the conclusion of each test, all data were written from RAM to the computer disk.

Prior calibration of the water depth sensors enabled measurements to be normalised to standard units of depth (mm) and rate (mm h^{-1}). As each depth sensor filled during a test, the sensitivity of the sensor decreased because of the shape of the calibration curve (Fig. 4). In order to optimise sensitivity (<0.8 mm) and capacity (~50%), the software was

Table 1
Kinetic energy distribution from the rainfall simulator for drop diameters of 5.1 and 2.7 mm

Fall height (m)	Drop size = 5.1 mm		Drop size = 2.7 mm	
	Velocity (m s^{-1})	Kinetic energy (J m^{-2} mm^{-1})	Velocity (m s^{-1})	Kinetic energy (J m^{-2} mm^{-1})
0.17	1.811	1.64	1.792	1.61
0.67	3.519	6.19	3.407	5.80
1.17	4.556	10.38	4.328	9.36
1.67	5.324	14.18	4.977	12.38
2.17	5.937	17.62	5.472	14.97
2.54	6.313	19.93	5.765	16.62

programmed to activate an alarm at 40 Hz, alerting the operator to the need to change or drain the sensor.

2.6. Performance of the simulator

The simulator delivered raindrops with energy varying from 1.6 to 19.9 J m^{-2} mm^{-1} (Table 1). Energy at the soil surface was calculated from the theory of Wang and Pruppacher (1977) using computer code that required drop size and fall height input data (Dr P. Kinnell, pers. comm., 1993). Kinetic energy was varied by changing the height of modules as well as excluding or including the plastic hypodermic needle cover.

Rainfall intensity was varied linearly, from below 40 to over 100 mm h^{-1}, by changing the rotation rate of the peristaltic pump (Fig. 6). Spatial variation in intensity across the test bed was very small, with coefficient of variation <5% at low rainfall intensities (<40
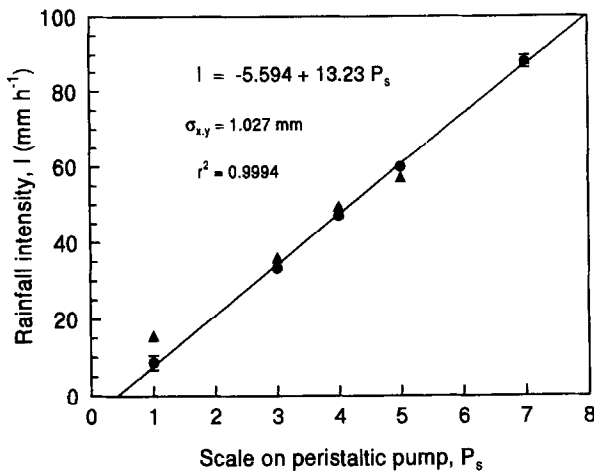

Fig. 6. Calibration of rainfall peristaltic pump (Masterflex 6–600 rpm): as a mean of all target sites ($n = 9$) (circles) and the values for the central, pluviometer position (triangles). The solid line shows the fitted calibration function for the mean data respectively. Error bars are 2 standard errors of the mean, which are generally smaller than the mean data symbols.
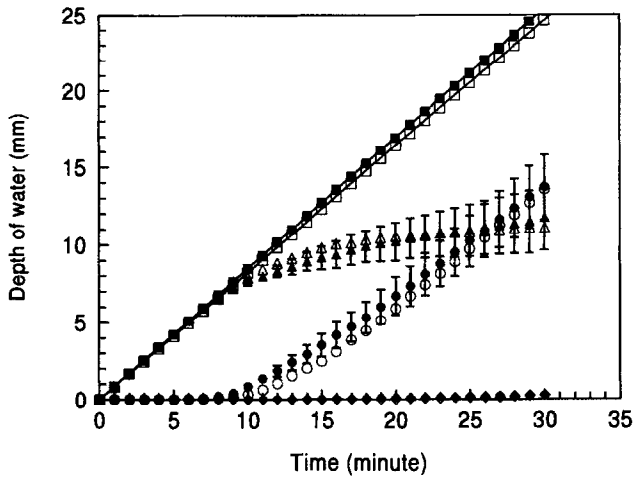
Fig. 7. Components of the hydrological balance: rainfall (square symbols), runoff (circles), infiltration (triangles) and drainage (diamonds) during a single run using simulated rainfall on air-dry soil with high energy rainfall (19.9 J m^{-2} mm^{-1}) and intensities of 50.7 mm h^{-1} (closed symbols) and 49.2 mm h^{-1} (open symbols). Mean drop diameter of rainfall was 5.1 mm. Error bars are 2 standard errors of the mean of eight replicated soil targets, which in some cases are smaller than the mean data symbols.

mm h^{-1}) and <3% at higher intensities. Fig. 6 shows that rainfall intensity at the centre of the bed (pluviometer position) was not significantly different from the mean rainfall intensity across the entire bed. Reproducibility in rainfall intensity from one test to another was also high (Fig. 7). Variation in intensity was within 2 mm h^{-1} for intensities of 50 mm h^{-1}, and approaching zero variation at high intensity (~70 mm h^{-1}).
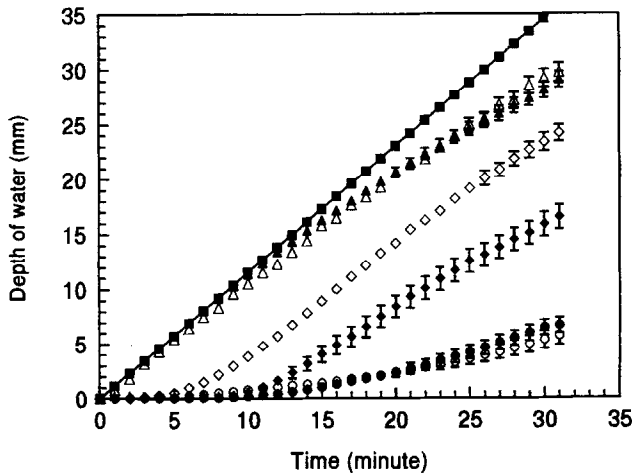

Fig. 8. Components of the hydrological balance: rainfall (square symbols), runoff (circles), infiltration (triangles) and drainage (diamonds) during a single run using simulated rainfall on air-dry (closed symbols) and pre-moistened soil (suction of 300 mm water) (open symbols). Rainfall energy was 1.64 J m^{-2} mm^{-1}, intensity 70 mm h^{-1} and mean drop diameter was 5.1 mm. Error bars are 2 standard errors of the mean, which in some cases are smaller than the mean data symbols.

Figs. 7 and 8 show examples of overall performance and reproducibility of the rainfall simulator and the aggregate bed at high ($19.9 \text{ J m}^{-2} \text{ mm}^{-1}$) and low ($1.6 \text{ J m}^{-2} \text{ mm}^{-1}$) kinetic energy, respectively. Low variation in rainfall enabled us to obtain high levels of reproducibility in measurement of infiltration and runoff between both samples within a test and between tests. Visual observation of surface ponding, seal condition, surface roughness and time to ponding and runoff indicated that the exchange bed behaved in a manner similar to that of the samples although no comparative measurements were made.

3. Discussion

The chronological detail made available by this simulator system allowed infiltration (the water passing through the soil surface) to be distinguished from drainage (the water draining from the base of the soil sample) over time. Provision of under-sample drainage simulated field soil behaviour more realistically than undrained samples. The formulation of the under-bed drainage base (1:1 diatomaceous earth and silica flour) allowed variation of drainage rate. Removal of ponded water on the surface allowed fuller development of rainfall–surface soil interactions than would be observed if ponding had been allowed to occur. Test samples were surrounded by an exchange bed, preventing the net export of particles from the test sample. The height of the rain module above the test bed and the drop size of the simulated rainfall allowed control of raindrop energy. Finally the control of delivery of water to the modules with a peristaltic pump allowed control of rainfall intensity. These features allowed us to investigate the behaviour of different soils exposed to a range of rainfall conditions without the limitations of rapid shielding of the soil surface by ponded water and the rapid saturation of the soil associated with small samples.

Some difficulty was experienced with lack of control of rainfall delivery at low intensity when the modules leaked air, particularly at low intensities when the modules were under suction. This proved to be a problem with the seal between the acrylic sheets failing due to the considerable stresses caused by water pressure and applied suction over the large surface area (0.5 m^2) of the module. Use of acrylic sheet for construction of the modules was not entirely satisfactory. Acrylic is known to swell when in contact with water and shrink on drying. This alternate expansion and contraction contributed to the deterioration of the rubber gasket and failure of glued joints. Some difficulties were also experienced with algal growth encouraged by the transparency of the module material. Some of these problems might be solved by using smaller modules ($500 \text{ mm} \times 500 \text{ mm} \times 40 \text{ mm}$) with interior reinforcement and constructed from opaque PVC sheeting.

4. Conclusions

A laboratory rainfall simulator was designed and constructed to deliver simulated rain to small soil samples under conditions where rainfall energy and intensity were controlled and runoff and drainage collected under conditions where no net loss of soil occurred from the test samples. Features of the simulator included hypodermic needle emitters, moving rainfall modules, small soil test samples surrounded by an exchange bed area, a regulated suction

on the base of the soil under test and rapid (1-min intervals), precise (<0.5 mm) and fully automated acquisition of accumulated rainfall, surface runoff and drainage.

The use of small samples with sub-drainage conditions enabled the measurement of surface aggregate breakdown without the complex effects of raindrop cushioning by ponded water and the multitude of interactions caused by flowing water on the sample surface. Use of electronic measuring cylinders of high sensitivity, with computer monitoring has provided a level of chronological detail not previously possible in this type of work. The properties of rain that are most important in understanding soil structural stability, total energy and energy flux density could be controlled in our rainfall simulator.

Acknowledgements

References

Eigel, J.D. and Moore, I.D., 1983. A simplified technique for measuring raindrop size and distribution. Trans. Am. Soc. Agric. Eng., 3: 1079–1084.

Gusli, S., Cass, A., MacLeod, D.A. and Hignett, C.T., 1995. Processes that distinguish hard setting from rain induced crusting. Proc. International Symposium on Sealing, Crusting, Hardsetting Soils: Productivity and Conservation. University of Queensland, Brisbane, Australia, 7–11 February 1994 (in press).

Hignett, C.T., 1991. Relating soil structure to runoff quality and quantity. International Hydrology and Water Resources Symposium, Perth, Australia, 2–4 October 1991. Institution of Engineers, Australia, 11 National Circuit, Barton, ACT 2600. Publication 91/22, pp. 301–305.

Horton, R.E., 1948. Statistical distribution of drop sizes and the occurrence of dominant drop sizes in rain. Trans. Am. Geophys. Union, 29: 642–630.

Kinnell, P., 1981. Rainfall intensity–kinetic energy relationships for soil loss prediction. Soil Sci. Soc. Am. J., 45: 153–155.

Kinnell, P., 1987. Rainfall energy in eastern Australia: intensity–kinetic energy relationships for Canberra, A.C.T. Aust. J. Soil Res., 25: 547–553.

Laws, J.O. and Parsons, D.A., 1943. Relation of raindrop size to intensity. Trans. Am. Geophys. Union, 24: 452–460.

Morin, J. and Benyamini, Y., 1977. Rainfall infiltration into bare soils. Water Resourc. Res., 13: 813–817.

Morin, J., Goldberg, D. and Seginer, I., 1967. A rainfall simulator with a rotating disk. Trans. Am. Soc. Agric. Eng., 10: 74.

Moss, A.J. and Watson, C.L., 1991. Rain impact soil crust. III. Effects of continuous and flawed crusts on infiltration, and the ability of plant covers to maintain crustal flaws. Aust. J. Soil Res., 29: 311–330.

Rosewell, C.J., 1986. Rainfall kinetic energy in eastern Australia. J. Climate Appl. Meteorol., 25: 1965–1968.

Ross, P.J., 1983. A water level sensor using a capacitance to frequency converter. J. Phys., E16: 827–828.

Wace, S.J. and Hignett, C.T., 1991. The effect of rainfall energy on tilled soils of different dispersion characteristics. Soil Tillage Res., 20: 57–67.

Walker, P.H., Hutka, J., Moss, A.J. and Kinnell, P.A., 1977. Use of a versatile experimental system for soil erosion studies. Soil Sci. Soc. Am. J., 41: 610–612.

Wang, P.K. and Pruppacher, H.R., 1977. Acceleration to terminal velocity of cloud and raindrops. J. Appl. Meteorol., 16: 275–280.